J. Mater. Environ. Sci. 7 (9) (2016) 3437-3446
ISSN : 2028-2508
CODEN: JMESC

Analytical and numerical modeling of the dispersion of particles in blood flow through elastic pipe

K. Gueraoui[2*], M. Taibi[2,5], M. Tricha[1,2], Y. Belkassmi[2], A. Elbouzidi[2], B. Bahrar[2], A. Mzerd[3], G. Zeggwagh[4]

[1]*Services de médecine physique et réadaptation, Hôpital militaire d'Instruction Mohamed V, Hay Ryad, Rabat, Morocco*
[2]*Team of modeling and simulating in mechanics and energeric, Faculty of Sciences, Mohammed V University, Rabat, Morocco*
[3]*Department of Physics, Faculty of Sciences, Mohamed V University, Rabat, Morocco*
[4]*Applied Mathematics Laboratory, Faculty of Sciences, Mohamed V University, Rabat, Morocco*
[5]*Laboratory of Mechanics and Energy, Faculty of Sciences Ain chock, Hassan II University-Casablanca, Morocco*

Received 22 Apr 2016, Revised 11 Jun 2016, Accepted 17 Jun 2016
**Corresponding author. E-mail: Kgueraoui@yahoo.fr (K. Gueraoui);*

Abstract
A numerical study concerning pulsatile flows of plastic fluids through isotropy elastic ducts is presented. The objective is to investigate the effects of elasticity of pipe wall material for an Ostwald fluid. An implicit volume method is used to solve the equations; we determine the pressure, the radial velocity, the axial velocity and the flow rate distributions. This study can be considered as a step in modeling of flow in blood vessels, may also contribute to other important fields such as water desalination or gel filtration.

Keywords: Pulsatile flow, Plastic fluid, dispersion, Numerical method, Isotropic elastic duct, Hemodynamic

Nomenclatures

w_0	:	Velocity characteristic of the flow in the axial direction;
$T_0 = \frac{2\pi}{\omega}$	:	The time tracking of the phenomenon;
L_0	:	Length of the conduit;
ω	:	Pulsation of the phenomenon;
η	:	Newtonian viscosity;
X_p	:	Position vector of the particle;
$\vec{V}_p$	:	Instantaneous velocity;
$R_e = \frac{\rho_0 . R_0 . w_0}{\eta}$	:	Reynolds number;
$\beta = R_0 \sqrt{\frac{\rho_0}{T_0 . \eta}}$	:	Womersley number.

1. Introduction
The vast majority of work on the deformable fluid flows in pipes is designed to model the blood flow in different sites of the vascular network. These both theoretical and experimental studies of blood flows lead to select three types of settings namely: - the parameters related to the nature of the fluid chosen to model the behavior of blood. These appear in the equation called the rheological behavior of the fluid, either obeys Newton's law [1] or laws to non - Newtonian type Casson [2], Ostwald [3], Quemada [4] or generalized Bingham [5]. -the parameters characterizing the nature and geometry of the duct wall where the flow occurs; they operate both in terms of fluid and in terms of the structure. They impose on the flow; fine modeling of real flows, though often taking account of simplifying assumptions, leads to very complex equations; these

complexities come mainly from the geometrical conditions which limit the flow [6-8] -the parameters related to hydrodynamic conditions [9-10]. The originality of this study comes from the simultaneous consideration of two-dimensional characters and non-permanent flow, taking into account the terms of inertia, the nonlinear behavior of the fluid (Ostwaldian fluid) and elastic character of the wall of the pipe. This approach, which only concerns the modeling of blood flow at the small circulation, is carried out by analytical and numerical means. The phenomena analyzed are related to periodic regimes. Numerical code developments enable us to study further the effect of the rheological parameters of the fluid and the wall on all of the flow. To illustrate these effects, we presented the evolution of pressure profiles and distributions of flow rate in the pipe.

2. Mathematical formulation

Modeling of blood flow is very delicate. In these flows takes place a large number of various kinds of parameters. One can describe the movement of a fluid such as blood by a set of partial differential equations derived from the fundamental laws of mechanics, that is to say, the laws of conservation of mass (continuity equation) the quantity of motion (momentum equation), to ask for a completely fluid dynamics problem. In the framework of our study, the fluid will be considered incompressible, non-Newtonian and the flow non-permanent and laminar.

3. Rheological behavior of the fluid

In our case the equations of conservation is written as follows:

Conservation of mass:

$$\frac{1}{r}\frac{\partial}{\partial r}[r.u]+\frac{\partial}{\partial z}[w]=0 \tag{1}$$

Momentum equation:

$$\frac{\partial \vec{v}}{\partial t}+(\vec{v}.\nabla).\vec{v}=-\frac{1}{\rho}\overrightarrow{div}(p)+\vec{f}+\frac{1}{\rho}\overrightarrow{div}(\tau) \tag{2}$$

4. Adimensionnalisation and simplification of equations

For the purpose of highlight dimensionless flow characteristics and whose order of magnitude for the intended application can measure the relative importance of different contributions, we introduce the following dimensionless quantities:

$$\hat{r}=\frac{r}{R_0} \qquad \hat{z}=\frac{z}{L_0} \qquad \hat{t}=\frac{t}{T_0} \qquad \hat{w}=\frac{w}{w_0} \qquad \hat{u}=\frac{u.L_0}{w_0.R_0}$$

$$\hat{\eta}_a=\frac{\eta_a}{\eta} \qquad \hat{P}_t=\frac{P_t.R_0^2}{\eta.w_0.L_0} \qquad \varepsilon=\frac{R_0}{L_0} \qquad R_e=\frac{\rho_0.R_0.w_0}{\eta} \qquad \beta=R_0\sqrt{\frac{\rho_0}{T_0.\eta}}$$

The continuity equation is written in the form:

$$\frac{1}{\hat{r}}\frac{\partial}{\partial \hat{r}}[\hat{r}.\hat{u}]+\frac{\partial}{\partial \hat{z}}[\hat{w}]=0 \tag{3}$$

The momentum equation:

$$\rho\frac{Du}{Dt}=-\frac{\partial p}{\partial r}+\frac{2}{r}\frac{\partial}{\partial r}\left(r.\eta_a.\frac{\partial u}{\partial r}\right)+\frac{\partial}{\partial z}\left(\eta_a\frac{\partial u}{\partial z}\right)-2\eta_a\frac{u}{r^2}+\frac{\partial}{\partial z}\left(\eta_a\frac{\partial w}{\partial r}\right)+\rho.f_r$$

$$\rho\frac{Dw}{Dt}=-\frac{\partial p}{\partial z}+\frac{1}{r}\frac{\partial}{\partial r}\left(r.\eta_a.\frac{\partial w}{\partial r}\right)+2\frac{\partial}{\partial z}\left(\eta_a\frac{\partial w}{\partial z}\right)+\frac{1}{r}\frac{\partial}{\partial r}\left(r.\eta_a.\frac{\partial u}{\partial z}\right)+\rho.f_z \tag{4}$$

In the framework of the application envisaged, the geometrical form factor ε is very small, so we can neglect the terms ε^2 or more, the terms $\mathrm{Re}\,\varepsilon$, and $\hat{f}_z$ as representing the force of gravity along the direction $\vec{z}$ can be assumed to be negligible.

In the case of a deformable wall and due to the variation of the geometric boundary of the flow following the axis $\overrightarrow{oz}$, it is more convenient to effect a change of variables as follows:

$$x=\frac{\hat{r}}{\hat{R}} \qquad \text{or} \qquad 0\le x\le 1$$

This system of equations is written as following:

$$\frac{1}{\hat{R}}\frac{1}{x}\frac{\partial\left(x\,\hat{u}^*\right)}{\partial\,x}+\frac{\partial\left(\hat{w}^*\right)}{\partial\,\hat{z}}-\frac{x}{\hat{R}}\left[\frac{\partial\,\hat{R}}{\partial\hat{z}}\frac{\partial\left(\hat{w}^*\right)}{\partial x}\right]=0 \tag{5}$$

$$\frac{\partial\,\hat{P}^*}{\partial x}=0 \tag{6}$$

$$\beta^2\frac{\partial\left(\hat{w}^*\right)}{\partial\,\hat{t}}-\frac{x}{\hat{R}}\left[\beta^2\frac{\partial\,\hat{R}}{\partial\hat{t}}\frac{\partial\,\hat{w}^*}{\partial x}\right]=-\frac{\partial\,\hat{p}}{\partial\hat{z}}+\frac{1}{\hat{R}^2}\frac{1}{x}\frac{\partial}{\partial x}\left[x.\hat{\eta}_a^*\left(\frac{\partial\,\hat{w}^*}{\partial x}\right)\right] \tag{7}$$

To the apparent viscosity, we adopt the model of Ostwald namely:

$$\hat{\eta}_a^*\frac{\partial\,\hat{w}^*}{\partial x}=\frac{k}{R^{m-1}}\left|\frac{\partial\,\hat{w}^*}{\partial x}\right|^{m-1}\frac{\partial\,\hat{w}^*}{\partial x} \tag{8}$$

5. Integrals equation system

The pressure gradient was unknown along the duct; the system of local equations can be solved separately, for it is added to it the system of integral equations of flow. By multiplying the local equations (5) and (7) by 2 *x* and integrating from 0 to 1, we obtain:

$$\beta^2\frac{\partial Q}{\partial t}=-\frac{\partial P}{\partial z}+\frac{2\beta^2}{R}\frac{\partial R}{\partial t}Q+\frac{2}{R}\tau_p \tag{9}$$

$$0=\mathrm{R}\frac{\partial Q}{\partial z}+\frac{2\beta^2}{R_e\varepsilon}\frac{\partial R}{\partial t}+2\frac{\partial R}{\partial z}Q \tag{10}$$

Where $Q=2\int_0^1 xw\,dx$ is the instantaneous overall flow rate through the section of the duct considered, and $\tau_p=\frac{1}{R}\left(\frac{\partial W}{\partial x}\right)_{x=1}$ the wall shear stress.

6. Dynamics of the particle

For the position of the particle, we have:
Determining the position of a spherical particle and assumed non-deformable well-defined size, moving inside the laminar and unsteady flow of the fluid under consideration, is obtained by integration of the following kinematic equation:

$$\frac{d\overrightarrow{X_p}}{dt}=\overrightarrow{V_p} \tag{11}$$

• For the momentum, we have:

The equation that we have adopted is that proposed by Odar and Hamilton to which we add the lift forces induced by shear [15], we get:

$$\frac{\pi D_p^3}{6}\rho_p\frac{d\vec{V}_p}{dt}=-\frac{1}{2}C_D\frac{\pi D_p^2}{4}\rho\left\|\vec{V}_p-\vec{V}\right\|\left(\vec{V}_p-\vec{V}\right)+\frac{\pi D_p^3}{6}\left(\rho_p-\rho\right)\vec{g}-C_A\rho\frac{\pi D_p^3}{6}\left(\frac{d\vec{V}_p}{dt}-\frac{d\vec{V}}{dt}\right) \tag{12}$$

The coefficient of acceleration C_A, is determined using the following equation [13-14]:

$$C_A=1.05-\frac{0.066}{A_C^2+0.12}$$

Or:

$$A_C=\frac{\left\|\vec{V}_p-\vec{V}\right\|^2}{D_p\left\|\frac{d\vec{V}_p}{dt}-\frac{d\vec{V}}{dt}\right\|^2}$$

The drag coefficient C_D, is a function of the Reynolds number R_{eg}, whether the slip of the smooth sphere is assumed. We have adopted, as part of our study, the wording proposed by Schiller and Newman [15]:

$$C_D=\frac{24}{R_{eg}}\left[1+0.15R_{eg}{}^{0.687}\right]$$

This relationship is valid for $R_{eg}<1000$

The projection, along the axes of the cylindrical coordinates, equations (5) and (6) lead to:

$$\frac{dX_{rp}}{dt} = V_{rp} \tag{13}$$

$$\frac{dX_{zp}}{dt} = V_{zp} \tag{14}$$

$$\frac{\pi D_P^3}{6}(\rho_P + C_A\rho)\frac{dU_p}{dt} = -\frac{1}{2}C_D\frac{\pi D_P^2}{4}\rho\left\|\vec{V}_p - \vec{V}\right\|\left(U_p - U\right) + C_A\rho\frac{\pi D_P^3}{6}\frac{dU}{dt} \tag{15}$$

$$\frac{\pi D_P^3}{6}(\rho_P + C_A\rho)\frac{dW_p}{dt} = -\frac{1}{2}C_D\frac{\pi D_P^2}{4}\rho\left\|\vec{V}_p - \vec{V}\right\|\left(W_p - W\right) + \frac{\pi D_P^3}{6}\left(\rho_P - \rho\right)g + C_A\rho\frac{\pi D_P^3}{6}\frac{dW}{dt} \tag{16}$$

Where: X_{rp}, X_{zp} are respectively radial and axial positions of the particle, U_p, W_p, the radial and axial velocities of the particle and U, W the radial and axial fluid velocity.

7. Method of resolution

The equations obtained previously do not admit analytical solutions, so the use of numerical methods appears mandatory. This method requires two steps: mesh and discretization [16-30].

- **Discretization**

The axial velocity:

By multiplying equation (7) by the volume of control (dxdz) and integrating along the length of time interval dt, it follows that:

$$\iiint \beta^2\frac{\partial\left(\hat{w}^*\right)}{\partial\hat{t}}dxd\hat{z}d\hat{t} - \iiint\frac{x}{\hat{R}}\left[\beta^2\frac{\partial\hat{R}}{\partial\hat{t}}\frac{\partial\hat{w}^*}{\partial x}\right]dxd\hat{z}d\hat{t} = -\iiint\frac{\partial\hat{p}}{\partial\hat{z}}dxd\hat{z}d\hat{t} + \iiint\frac{1}{\hat{R}^2}\frac{1}{x}\frac{\partial}{\partial x}\left[x.\hat{\eta}_a^*\left(\frac{\partial\hat{w}^*}{\partial x}\right)\right]dxd\hat{z}d\hat{t}$$

The equation can therefore be written in the following form:

$$A(i,j)\hat{W}^{*\,dt+t}_{(i,j)} + B(i,j)\hat{W}^{*\,dt+t}_{(i+1,j)} + C(i,j)\hat{W}^{*\,dt+t}_{(i-1,j)} = D(i,j) \tag{17}$$

With:

$$A(i,j) = \beta^2\Delta x\Delta\hat{z} + \frac{1}{\hat{R}_p{}^2}\frac{1}{x_p\Delta x}\left[x_e.\hat{\eta}_a^*\right)_e + x_o.\hat{\eta}_a^*\right)_o\Delta\hat{z}\Delta\hat{t}$$

$$B(i,j) = -\beta^2\frac{x_p}{2\hat{R}_p}\left(\frac{\partial\hat{R}}{\partial\hat{t}}\right)_p^t\Delta\hat{z}\Delta\hat{t} - \frac{1}{\hat{R}_p{}^2}\frac{1}{x_p\Delta x}x_e.\hat{\eta}_a^*\right)_e\Delta\hat{z}\Delta\hat{t}$$

$$C(i,j) = \beta^2\frac{x_p}{2\hat{R}_p}\left(\frac{\partial\hat{R}}{\partial\hat{t}}\right)_p^t\Delta\hat{z}\Delta\hat{t} - \frac{1}{\hat{R}_p{}^2}\frac{1}{x_p\Delta x}x_o.\hat{\eta}_a^*\right)_o\Delta\hat{z}\Delta\hat{t}$$

$$D(i,j) = -\left(\frac{\partial\hat{p}}{\partial\hat{z}}\right)_p^{dt+t}\Delta x\Delta\hat{z}\Delta\hat{t} + \beta^2\Delta x\Delta\hat{z}\hat{w}^{*\,t}_{\ p}$$

The velocity of the flow

By applying the volume differences method for equation (9), the algebraic equation can therefore be written in the following form:

$$Q_{(j)}^{t+dt} = \left(-\frac{\partial P}{\partial z}\right)_{(j)}^t + \frac{2}{R}\tau_p\Big)_{(j)}^t + \frac{\beta^2}{\Delta t}Q_{(j)}^t\Bigg)\Bigg/\left(\frac{\beta^2}{\Delta t} - \frac{2\beta^2}{R}\frac{\partial R}{\partial t}\right)_{(j)}^t \tag{18}$$

The radius of the conduit:

By applying the volume differences method for equation (10), we obtain:

$$\left(\frac{Q_{(j)}^{t+dt}}{\Delta z}\right)R_{(j+1)}^{t+dt} + \left(\frac{2\beta^2}{R_e\varepsilon\Delta t} + \frac{Q_{(j+1)}^{t+dt} - Q_{(j-1)}^{t+dt}}{2\Delta z}\right)R_{(j)}^{t+dt} + \left(-\frac{Q_{(j)}^{t+dt}}{\Delta z}\right)R_{(j-1)}^{t+dt} = 0 \tag{19}$$

The pressure:
The pressure is determined using the following equation:

$$P(j) = \frac{R(j) - R_0}{\alpha} + P_{ext}$$

The position of the particle:
The equation (13) becomes:

$$\frac{dX_{rp}}{dt} = f(X_{rp})$$

With: $f(X_{rp}) = V_{rp}$

According to the Runge-Kutta method, this equation becomes:

$$X_{rp\ (i,j)}^{\ dt+t} = X_{rp\ (i,j)}^{\ t} + \Delta t.f(X_{rp(i,j)}^{\ t+dt/2})$$

Or:

$$X_{rp\ (i,j)}^{\ t+dt/2} = X_{rp\ (i,j)}^{\ t} + \frac{\Delta t}{2}.f\left(X_{rp\ (i,j)}^{\ t}\right)$$

With: $f\left(X_{rp\ (i,j)}^{\ t}\right) = V_{rp\ (i,j)}^{\ t}$

And:

$$f\left(X_{rp\ (i,j)}^{\ t+\Delta t/2}\right) = V_{rp\ (i,j)}^{\ t}$$

- Equation (14) becomes:

$$\frac{dX_{zp}}{dt} = f(X_{zp})$$

With: $f(X_{zp}) = V_{zp}$

According to the Runge-Kutta method, this equation is:

$$X_{zp\ (i,j)}^{\ dt+t} = X_{zp\ (i,j)}^{\ t} + \Delta t.f(X_{zp(i,j)}^{\ t+dt/2})$$

Or:

$$X_{zp\ (i,j)}^{\ t+dt/2} = X_{zp\ (i,j)}^{\ t} + \frac{\Delta t}{2}.f\left(X_{zp\ (i,j)}^{\ t}\right)$$

With: $f\left(X_{zp\ (i,j)}^{\ t}\right) = V_{zp\ (i,j)}^{\ t}$

And:

$$f\left(X_{zp\ (i,j)}^{\ t+\Delta t/2}\right) = V_{zp\ (i,j)}^{\ t}$$

- Equation (15) becomes:

$$\frac{dU_p}{dt} = f(U_p)$$

With:

$$f(U_p) = \left[-\frac{1}{2}C_D\frac{\pi D_P^2}{4}\rho\left\|\vec{V}_p - \vec{V}\right\|\left(U_p - U\right) + C_A\rho\frac{\pi D_P^3}{6}\frac{dU}{dt}\right] / \left(\frac{\pi D_P^3}{6}(\rho_P + C_A\rho)\right)$$

According to the Runge-Kutta method, this equation is:

$$U_{p\ (i,j)}^{\ t+dt} = U_{p\ (i,j)}^{\ t} + \Delta t.f(U_{p\ (i,j)}^{\ t+dt/2})$$

With:

$$U_{p\ (i,j)}^{\ t+dt/2} = U_{p\ (i,j)}^{\ t} + \frac{\Delta t}{2}.f(U_{p\ (i,j)}^{\ t})$$

$$f\left(U_{p\,(i,j)}^{\,t+dt/2}\right)=\left[-\frac{1}{2}C_D\frac{\pi D_P^2}{4}\rho\left\|\vec{V}_p-\vec{V}\right\|\left(U_{p\,(i,j)}^{\,t+dt/2}-U\right)+C_A\rho\frac{\pi D_P^3}{6}\frac{dU}{dt}\right]/\left(\frac{\pi D_P^3}{6}(\rho_P+C_A\rho)\right)$$

And:

$$f\left(U_{p\,(i,j)}^{\,t}\right)=\left[-\frac{1}{2}C_D\frac{\pi D_P^2}{4}\rho\left\|\vec{V}_p-\vec{V}\right\|\left(U_{p\,(i,j)}^{\,t}-U\right)+C_A\rho\frac{\pi D_P^3}{6}\frac{dU}{dt}\right]/\left(\frac{\pi D_P^3}{6}(\rho_P+C_A\rho)\right)$$

- Equation (16) becomes:

$$\frac{\pi D_P^3}{6}(\rho_P+C_A\rho)\frac{dW_p}{dt}=-\frac{1}{2}C_D\frac{\pi D_P^2}{4}\rho\left\|\vec{V}_p-\vec{V}\right\|(W_p-W)+\frac{\pi D_P^3}{6}(\rho_P-\rho)g+C_A\rho\frac{\pi D_P^3}{6}\frac{dW}{dt}$$

With: $\frac{dW_p}{dt}=f(W_p)$

or:

$$f(W_p)=\left[-\frac{1}{2}C_D\frac{\pi D_P^2}{4}\rho\left\|\vec{V}_p-\vec{V}\right\|(W_p-W)+\frac{\pi D_P^3}{6}(\rho_P-\rho)g+C_A\rho\frac{\pi D_P^3}{6}\frac{dW}{dt}\right]/\left(\frac{\pi D_P^3}{6}(\rho_P+C_A\rho)\right)$$

According to the Runge-Kutta method, this equation is:

$$W_{P\,(i,j)}^{\,t+dt}=W_{P\,(i,j)}^{\,t}+\Delta t.f\left(W_{P\,(i,j)}^{\,t+dt/2}\right)$$

And:

$$W_{P\,(i,j)}^{\,t+dt/2}=W_{P\,(i,j)}^{\,t}+\frac{\Delta t}{2}.f\left(W_{P\,(i,j)}^{\,t}\right)$$

With:

$$f\left(W_{p\,(i,j)}^{\,t}\right)=\left[-\frac{1}{2}C_D\frac{\pi D_P^2}{4}\rho\left\|\vec{V}_p-\vec{V}\right\|\left(W_{p\,(i,j)}^{\,t}-W\right)+\frac{\pi D_P^3}{6}(\rho_P-\rho)g+C_A\rho\frac{\pi D_P^3}{6}\frac{dW}{dt}\right]/\left(\frac{\pi D_P^3}{6}(\rho_P+C_A\rho)\right)$$

And:

$$f\left(W_{p\,(i,j)}^{\,t+dt/2}\right)=\left[-\frac{1}{2}C_D\frac{\pi D_P^2}{4}\rho\left\|\vec{V}_p-\vec{V}\right\|\left(W_{p\,(i,j)}^{\,t+dt/2}-W\right)+\frac{\pi D_P^3}{6}(\rho_P-\rho)g+C_A\rho\frac{\pi D_P^3}{6}\frac{dW}{dt}\right]/\left(\frac{\pi D_P^3}{6}(\rho_P+C_A\rho)\right)$$

8. Results

In Figure 1, we illustrate the pressure distribution for two values of the fluid behavior index, n = 0.68 and n = 1, corresponding to an Ostwald fluid for the first and for a Newtonian fluid for the second.
It can be seen that a decrease of n, resulting in a more pronounced shear thinning, is accompanied by a decrease in apparent viscosity resulting in a decrease of the pressure values. We find similar results to those obtained by other authors [11-12, 16].

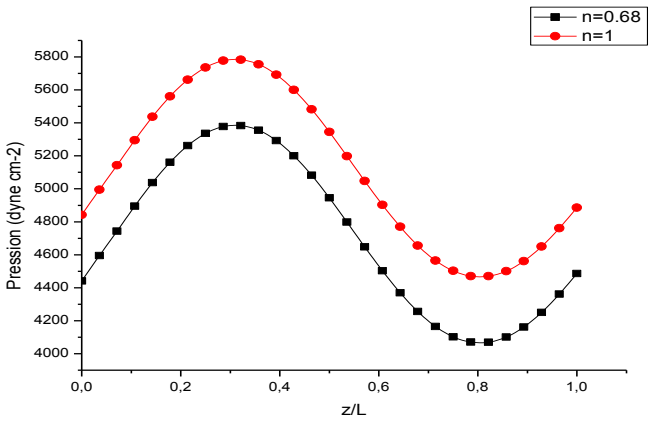

Figure 1: The pressure profiles as a function of the axial variable, *z*, at time *T / 2* for two values of the behavior index of the fluid, n

In Figure 2, we have illustrated the flow rate profile for two values of the fluid behavior index, n = 0.68 and n = 0.54.
It can be seen that a decrease of n, resulting in a more pronounced shear thinning, is accompanied by a decrease in apparent viscosity resulting in an increase of the values of the flow rate. We find qualitatively similar results to those obtained by other authors [11, 16].

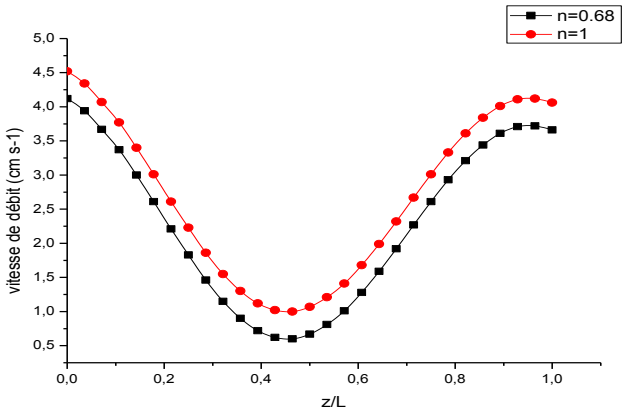

Figure 2: Profile of the flow rate as a function of the axial variable, *z*, at time *T / 2* for two values of the behavior index of the fluid, n

In Figure 3 is shown the profile of pressure, there is an increase in the consistency of the fluid, k, which causes an increase in apparent viscosity resulting in an increase in pressure values. These results are qualitatively similar to those obtained by other authors [11-12].

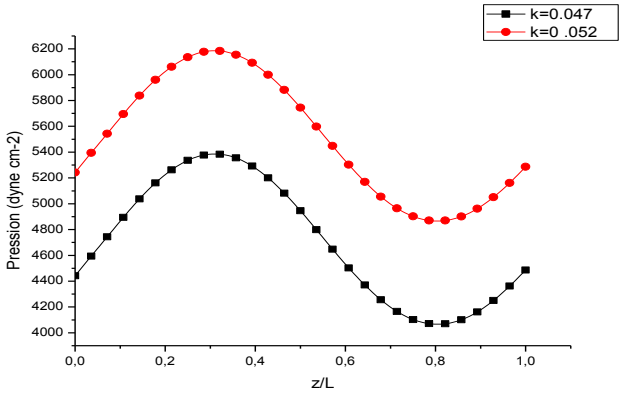

Figure 3: the pressure profiles as a function of the axial variable, *z*, at time *T / 2* for two values of the consistency of the fluid, *K*.

In figure 4, there is a decrease in the consistency of the fluid leads to an increase of values of the flow rate during a period.

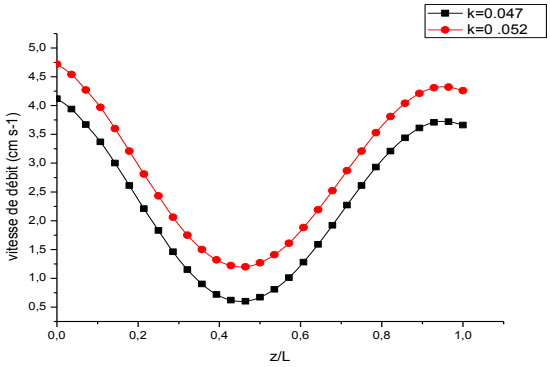

Figure 4: Profiles of the flow rate as a function of the axial variable, *z*, at time *T / 2* for two values of the consistency of the fluid, *K*

The 5 and 6 show the evolution of the pressure profile and flow rate for two values of the angle of the cone Ψ = 0.015 rd and Ψ = 0.025 = 0.015 rd.

We can see in figure 5, a decrease in Ψ causes a reduction of pressure values during a period, but in figure 6, we can note that the values of the flow rate increase when Ψ decreases. This is due to the increase of the section of tube.

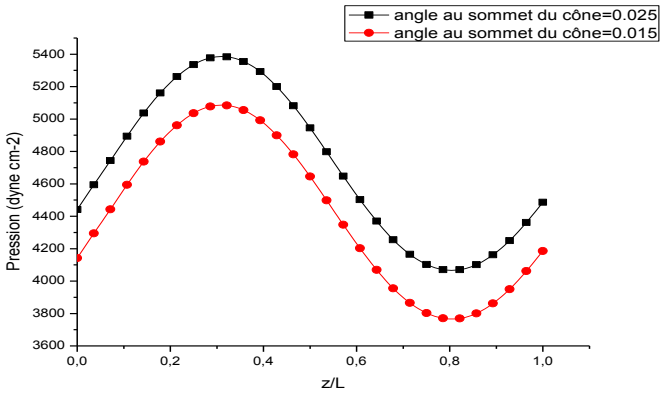

Figure 5: The pressure profiles as a function of the axial variable, *z*, at time *T / 2* for two values of the apex angle of the cone, Ψ

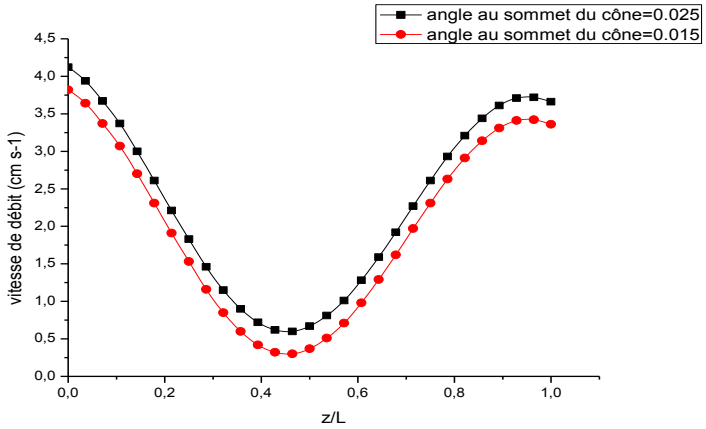

Figure 6: Profiles of the flow rate as a function of the axial variable, *z*, at time *T / 2* for two values of the apex angle of the cone, Ψ

We study in figures 7 and 8 the influence of the elasticity of the wall on the pressure distribution and the flow rate.
It is noted that an increase of elasticity coefficient of the wall results in a decrease of the Young's modulus in a period, and therefore to a greater deformability of the wall and therefore to an increase in pressure values and the flow rate. These results are qualitatively similar to those obtained by other authors [9].

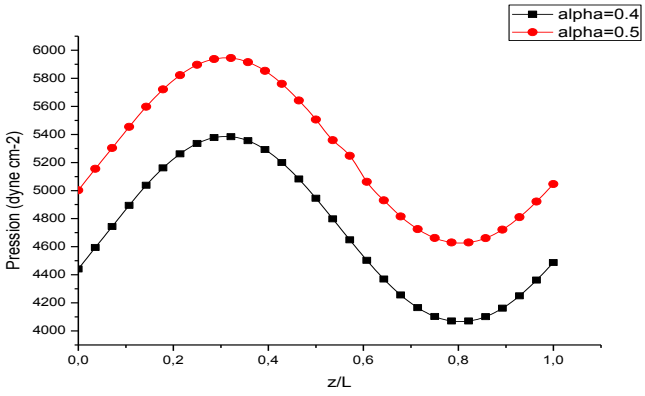

Figure 7: Pressure profiles in function of the axial variable, *z*, at time *T / 2* for two values of the coefficient of elasticity of the wall, α

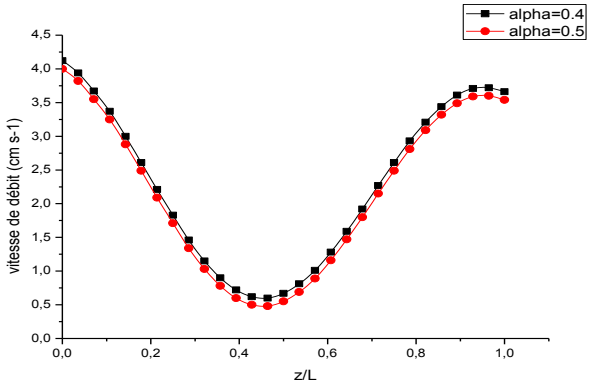

Figure 8: Flow velocity profiles as a function of the axial variable, *z*, at time *T / 2* for two values of the coefficient of elasticity of the wall, α

Conclusion

The objective we have set for ourselves consisted in proposing a model of mono-phase flow of non-Newtonian fluid in conduct with elastic wall. This study focuses on applications that can be made in hemodynamic more particularly in the microcirculatory system. Theoretical and numerical studies using Volume differences method implicit scheme were used to determine the pressure profile and the profile of the pipe with elastic wall.

We studied the influence of rheological parameters of the fluid (K consistency and behavior index n), and rheological parameters of the duct (α coefficient of elasticity of the wall, Ψ the apex angle of the cone). One can able to discern the importance of these parameters on the flow in a part of the microcirculatory system. But, we must note that many more research is needed to deal satisfactorily a subject of such importance. Indeed, we limited ourselves to the consideration of an elastic and impermeable pipe wall.

References

1. Hammoumi A., Kerroum M., Gueraoui K., Zeggwagh G., Modélisation théorique d'écoulements non permanents de fluides à comportement Newtonien en conduites poreuses à paroi viscoélastique. Application à la circulation sanguine. *Actes Inst. Agron. Veto (Maroc)* 13 (2) (1993) 41-50.
2. Casson N., *A flow equation for pigment oil suspensions of printing ink type. In: Rhoelogy of disperse systems Ed. Mill C.C., Pergamon London* (1959) 84-102.
3. Bellet D., *Relations entre comportements rhéologiques pseudoplastiques et échanges thermiques. Thèse de Doctorat Es-Sciences, U.P.S, Toulouse* (1973).
4. Quemada D., Rheology of concentrated disperse systems. 3- General feactures of the proposed non newtonian model. Comparison with experimental data. *Rheol Acta* 17 (1978) 643-653.
5. Gueraoui K., Hammoumi A, Zeggwagh G, Modélisation théorique d'écoulements pulsés de fluides non newtoniens en conduites viscoélastiques poreuses et anisotropes. *Acad Sci*, 2 (1998) 561-568.
6. Ly D.P., Bellet D., Bousquet A., Boyer P., *Ecoulements pulsés de fluides inélastiques en conduites tronconique ou déformable. Revue de Physique Appliquée* 16 (1981) 323-331.
7. Bitoun J.P., *Etudes théorique et expérimentale de la microcirculation sanguine au passage d'une sténose. Thèse de Doctorat de l'LN.P, Toulouse* (1985).
8. Rakotomalala A.R., Bellet D., Ecoulements transitoires et périodiques de fluides non newtoniens en conduites tronconiques. *Journal de Physique 1* (1991) 87-102.
9. Bahrar B., *Influence, sur les écoulements transitoires en conduite, des termes d'inertie de la paroi, ainsi que des déformations de flexion et de cisaillement*. Thèse de Doctorat de 3° cycle, LN.S.A, (1986) Lyon.
10. Rakotomalala A.R., *Ecoulements non newtoniens en conduites rigides et déformables. Thèse de Doctorat Es-Sciences, LN.P, Toulouse* (1989).
11. Gueraoui K., Hammoumi A., Zcggvvagh G., *A numerical solution of pulsatile flow of an inelastic fluid through anisotropic porous viscoelastic pipes Houille Blanch* (1998) 13-20.
12. Gueraoui K., Taibi M., Ghouli A., Mrabti A., Zeggwagh G., Haddad Y., Pulsating flow of inelastic fluids in anisotropic porous viscoelastic tubes. *International Review of Mechanical Engineering*, 2 (2008) 506-512.

13. Wells M.R., Stock D.E., The effects of crossing trajectories on the dispersion of particules in a turbulent flow. *J. Fluid Mech.*, 136 (1983) 31-62.
14. Oesterlé B., *Etude des caratéristiques locales d'un écoulement gaz-solide en suspension diluée. Transferts cinétiques dans la phase solide. Thèse d'Etat soutenue à l'Université de Nancy 1*, (1986).
15. Saad A., Echchelh A., Lahlou F., Gueraoui K., Cardot P., The kinematic elution of ^{99m}Tc radio labeled red blood cells in a channel of gravitational field flow fractionation (GrFFF). *International Review of Mechanical Engineering*, 2(2) (2008) 233-240.
16. Chammami R., Taibi M., Hami M., Gueraoui K., Zeggwagh G., *Influence of the kind of duct on two-fluid pulsatile flows model. Application to the microcirculation, Houille Blanche* (2001) 18-24.
17. Taibi M., Chammami R., Kerroum M., Gueraoui K., El Hammoumi A., Zeggwagh G., *Pulsating flow of two phases in deformable or rigide tubes, ITBM-RBM* 23 (2002) 149-158.
18. Driouich A, Gueraoui K., Haddad Y.M., Hammoumi A., Kerroum M., Fihri O.F., *Mathematical modeling of non permanent flows of molten polymers, International Review of Mechanical Engineering (IREME),* 4 (6) (2010) 689-694.
19. El-tourroug H., Gueraoui K., Hassanain N., Driouich M., Men-La-Yakhaf S., *Numerical Modeling of the Phenomenon of Crystallization of Incompressible Fluid Flows into Rigid Pipes. Application to Polymer Melts. International Review on Modelling and Simulations (IREMOS),* 8(1) (2015), 99-103.
20. Belcadi M., El Rhaleb H., Gueraoui K., Driouich M., *Hybridization microwave and laser for melting of ceramic surface, Adv. Studies Theo. Phys.*, 8 (2014).
21. Aberdane I., Gueraoui K., Taibi M., Ghouli A., El-Hammoumi A., Cherraj M., Kerroum M., Walid M., Fihri O.F., Haddad Y.M., Two-dimensional theoretical and numerical approach of pollutant transport in the lowest layers of the atmosphere, *International Review of Mechanical Engineering (IREME),* 3(4), (2009) 494-502.
22. Sammouda M., Gueraoui K., Driouich M., El Hammoumi A., Brahim A.I., *The variable porosity effect on the natural convection in a non-darcy porous media, International Review on Modelling and Simulations (IREMOS),* 4 (5) (2011) 2701-2707.
23. Driouich M., Gueraoui K., Sammouda M., Haddad M.Y., A New Numerical Code to Study the Flow of Molten Polymers In Elastic Pipes. AES-ATEMA International Conference Series - *Advances and Trends in Engineering Materials and their Applications,* (2011).
24. Driouich M., Gueraoui K., Sammouda M., Haddad Y. M., Aberdane I, *The Effect of Electric Field on the Flow of a Compressible Ionized Fluid in a Cylindrical Tube. Adv. Studies Theor. Phys.*, 6 (2012) 687-696
25. Driouich M., Gueraoui K., Sammouda M., Haddad Y.M., The Effect of the Rheological Characteristics of the Molten Polymer on its Flow in Rigid Cylindrical Tubes, *Adv. Studies Theor. Phys.*,6 (2012) 569-586
26. Sammouda M., Gueraoui K., Driouich M., El-Hammoumi A., Iben Brahim A., *Non-Darcy natural convection heat transfer along a vertical cylinder filled by a porous media with variable porosity, International Review of Mechanical Engineering (IREME),* 6 (4),(2012) 698-704.
27. Sammouda M., Gueraoui K., Driouich M., Ghouli A., Dhiri A., *Double diffusive natural convection in non-darcy porous media with non-uniform porosity, International Review of Mechanical Engineering (IREME),* 7 (6) (2013) 1021-1030.
28. El Khaoudi F., Gueraoui K., Driouich M., Sammouda, *M., Numerical and theoretical modeling of natural convection of nanofluids in a vertical rectangular cavity, International Review on Modelling and Simulations (IREMOS),* 7 (2),(2014) 350-355. http://dx.doi.org/10.15866/iremos.v7i2.585
29. Men-La-Yakhaf S., Gueraoui K., Driouich M., *New numerical and mathematical code reactive mass transfer and heat storage facilities of argan waste. Advanced Studies in Theoretical Physics*, 8(10) (2014) 485 – 498. http://dx.doi.org/10.15866/ireme.v8i1.1265
30. Men-la-yakhaf S., Gueraoui K., Maaouni A., Driouich M., *Numerical and mathematical modeling of reactive mass transfer and heat storage installations of argan waste, International Review of Mechanical Engineering (IREME),* 8 (1) (2014) 236-240.http://dx.doi.org/10.15866/ireme.v8i1.1265
31. Tricha M., Gueraoui K., Zeggwagh G., Mzerd A., *New Numerical and Theoretical Approaches to Study the Blood Flows at Microcirculation Level. International Review of Mechanical Engineering (IREME),* 8(6) (2014) 1043-1046. http://dx.doi.org/10.15866/ireme.v8i6.2725